

Self-Assembly of Metallo-Supramolecules with Dissymmetrical Ligands and Characterization by Scanning Tunneling Microscopy

Junjuan Shi,[#] Yiming Li,[#] Xin Jiang, Hao Yu, Jiaqi Li, Houyu Zhang, Daniel J. Trainer, Saw Wai Hla, Heng Wang, Ming Wang,* and Xiaopeng Li*



Cite This: *J. Am. Chem. Soc.* 2021, 143, 1224–1234



Read Online

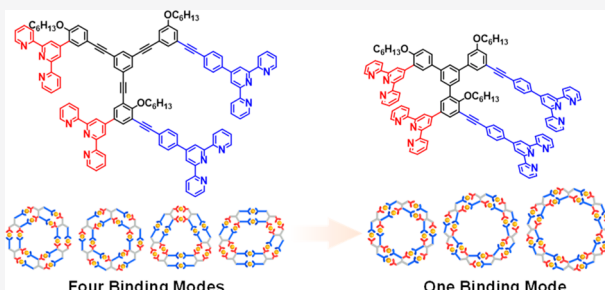
ACCESS |

Metrics & More

Article Recommendations

Supporting Information

ABSTRACT: Asymmetrical and dissymmetrical structures are widespread and play a critical role in nature and life systems. In the field of metallo-supramolecular assemblies, it is still in its infancy for constructing artificial architectures using dissymmetrical building blocks. Herein, we report the self-assembly of supramolecular systems based on two dissymmetrical double-layered ligands. With the aid of ultra-high-vacuum, low-temperature scanning tunneling microscopy (UHV-LT-STM), we were able to investigate four isomeric structures corresponding to four types of binding modes of ligand LA with two major conformations complexes A. The distribution of isomers measured by STM and total binding energy of each isomer obtained by density functional theory (DFT) calculations suggested that the most abundant isomer could be the most stable one with highest total binding energy. Finally, through shortening the linker between inner and outer layers and the length of arms, the arrangement of dissymmetrical ligand LB could be controlled within one binding mode corresponding to the single conformation for complexes B.



INTRODUCTION

Nature has developed impeccable systems for precise self-assembly of well-organized bioarchitectures with desirable functions. Inspired by nature, chemists have endeavored to design and construct supramolecular structures with various functions over the past decades.^{1,2} Among them, coordination-driven self-assembly is a well-documented methodology for preparing metallo-supramolecules with precisely controlled shapes and sizes.³ Indeed a variety of 2D and 3D metallo-supramolecules have been achieved.^{4–18} Most of these structures, which have highly symmetrical shapes and geometries, were obtained by self-assembly of symmetrical ligands, due to the high predictability and controllability for ultimate assemblies provided by the symmetrical building blocks. Meanwhile, symmetrical ligands can effectively avoid the generation of unexpected structures with similar thermodynamic stability, especially for the self-assembly of multiple ligands.

Asymmetrical and dissymmetrical structures are widespread and play a critical role in nature and life systems. For example, the dissymmetrical structures of proteins are crucial for many specific functions of the cell.¹⁹ To date, however, very few metallo-supramolecules were obtained by assembly of dissymmetrical ligands but were limited to small sizes and simple structures.²⁰ Particularly, there exist three major challenges in metallo-supramolecular systems based on dissymmetrical ligands. First, the building blocks with low symmetry are usually

difficult to prepare due to the multistep synthesis and tedious purification. Moreover, because of the uncertain orientation of each building block, multiple isomers could be generated during self-assembly with similar physical properties and, thus, hindering further isolation. Finally, even if the assembly with a predominant arrangement is obtained, the characterization of such complicated structures with dissymmetrical ligands would remain a formidable challenge.

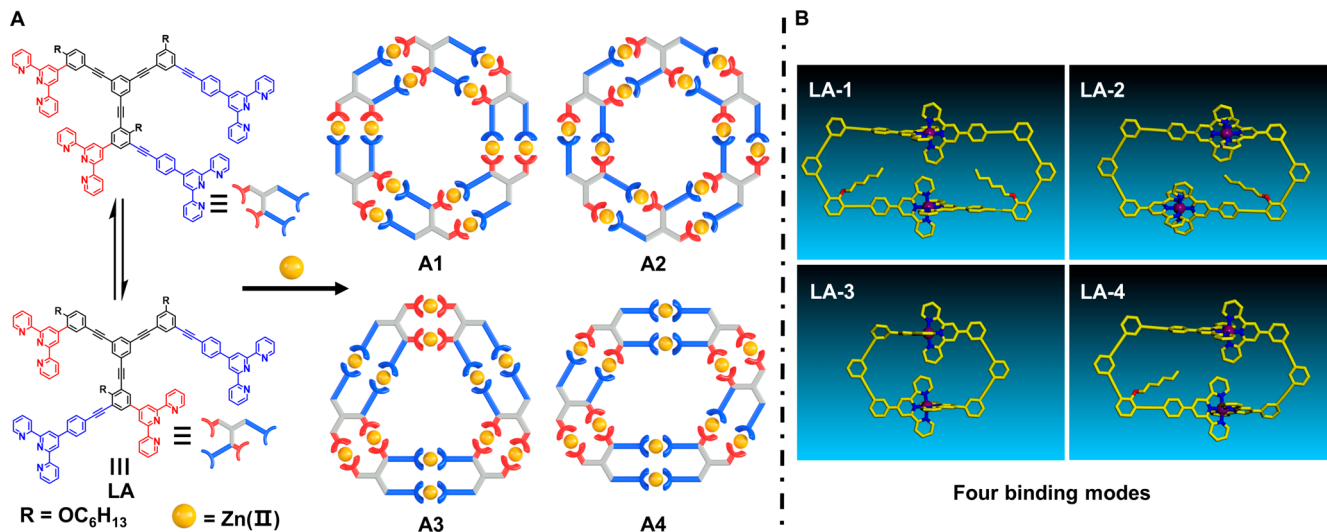
In the past decades, conventional characterization techniques like NMR, electrospray ionization–mass spectrometry (ESI–MS), traveling wave ion mobility–mass spectrometry (TWIM–MS), and single-crystal X-ray diffraction have been well established for characterizing supramolecules constructed by highly symmetrical building blocks with large sizes and complex structures.^{10b,13c,15b,21} However, these techniques become less effective in investigating supramolecules assembled by dissymmetrical ligands. For instance, the increased chemical environments caused by the low symmetry would significantly broaden the NMR signals and make the spectrum obscure. Furthermore, if all the isomeric structures with the same charges have similar

Received: December 1, 2020

Published: January 4, 2021



Scheme 1. (A) Self-Assembly of Dissymmetrical Ligand LA for the Construction of Complexes A Corresponding to Four Isomers Based on Four Binding Modes and Two Major Conformations of LA and (B) Modeling Structures of Four Binding Modes in Complexes A



structural collision cross sections, TWIM-MS is unable to distinguish those isomers. In crystallographic analysis, the isomers constructed by dissymmetrical ligands usually lead to uncertain and irregular packing of supramolecules. As such, only one or few isomers could crystallize out of a mixture of isomers in the solutions. Therefore, effective characterization techniques are highly demanded for investigating the supramolecules with dissymmetrical ligands. In recent years, scanning tunneling microscopy (STM) has emerged as a powerful tool to characterize supramolecular assemblies, since it can directly image each individual structure at submolecular resolution and reflect the population of each isomer in the complex system.²²

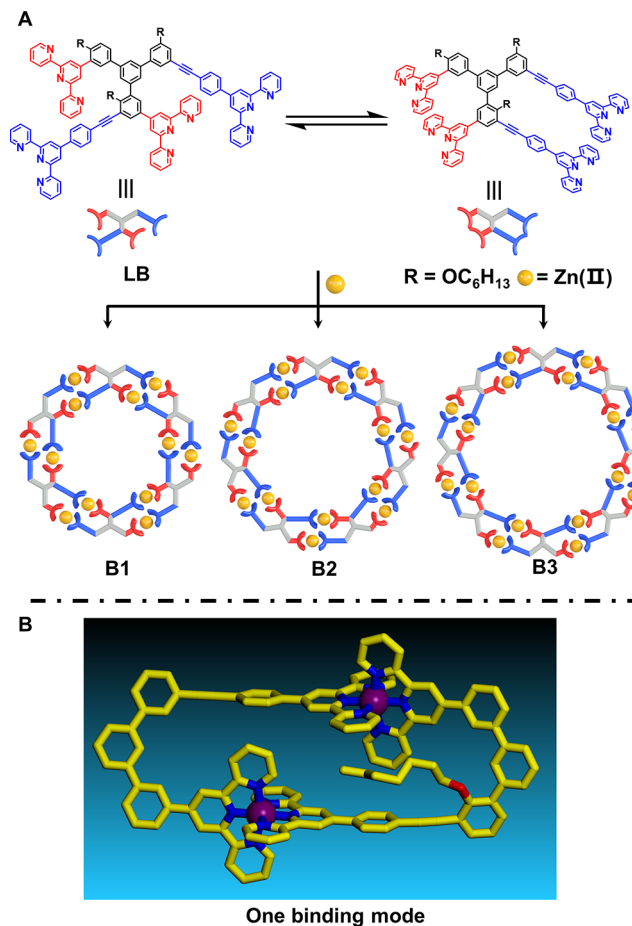
Among coordination-driven self-assembly, 2,2':6',2"-terpyridine (tpy) has been widely used as a versatile building block for constructing various symmetrical supramolecular architectures.^{9c,e,10a,21g,23} In addition, the octahedral structures of the \langle tpy-M-tpy \rangle coordination sites with ca. 1 nm height on surface have higher electron density than the flat organic skeletons; thus, they can be clearly distinguished in STM and facilitate imaging the structure and conformation of metallo-supramolecules.^{23e,f} Herein, we reported the design, synthesis, and self-assembly of two dissymmetrical tetratopic tpy ligands (LA and LB) with Zn(II). In our design, by adjusting the distance between inner and outer layers of the ligands and the length of arms, the symmetry and isomeric structures of the supramolecules are expected to be controlled by the steric hindrance generated during the self-assembly process. STM was utilized to investigate the isomeric structure and obtain the distribution of each isomer. The results showed that loose ligand LA generated four hexameric isomers with the same composition as we expected based on four types of binding modes during self-assembly (**Scheme 1**). In comparison, the compact ligand LB self-assembled into a mixture of hexamer, heptamer, and octamer (**Scheme 2**) with only one coordination mode because of the steric hindrance between the two layers.

■ RESULT AND DISCUSSION

Synthesis and Self-Assembly of Complexes A with Four Binding Modes Followed by NMR and Mass Spectrometry Characterization.

LA was synthesized via a

Scheme 2. (A) Self-Assembly of Dissymmetrical Ligand LB for the Construction of Complexes B1–B3 for Hexamer, Heptamer, and Octamer, Respectively, with One Binding Mode and (B) Modeling Structure of the Binding Mode in Complexes B



multifold Sonogashira coupling reaction and purified by column chromatography (the synthetic route is shown in **Scheme S1** in

the Supporting Information). All of the precursors and ligand were fully characterized by NMR (^1H , ^{13}C , COSY, and NOESY), ESI-MS, and MALDI-TOF mass spectrometry (see details in the Supporting Information). The supramolecules A were successfully prepared by mixing ligand LA and Zn(II) with an exact stoichiometric ratio of 1:2 in $\text{CHCl}_3/\text{CH}_3\text{OH}$ solution at 50 °C for 12 h, followed by the addition of an excessive amount of NH_4PF_6 to obtain a yellow precipitate in high yield. It is worth noting that, because of the dissymmetrical feature, LA could have two major conformations, which lead to four types of binding modes and generate four isomers during self-assembly (Scheme 1).

The double-layered metallocycles were first characterized by ^1H NMR spectroscopy. Due to the existence of multiple isomeric components and slow tumbling motion of supramolecules on the NMR time scale, broadening signals were observed in the ^1H NMR spectrum (Figure 1B and Figure S97).

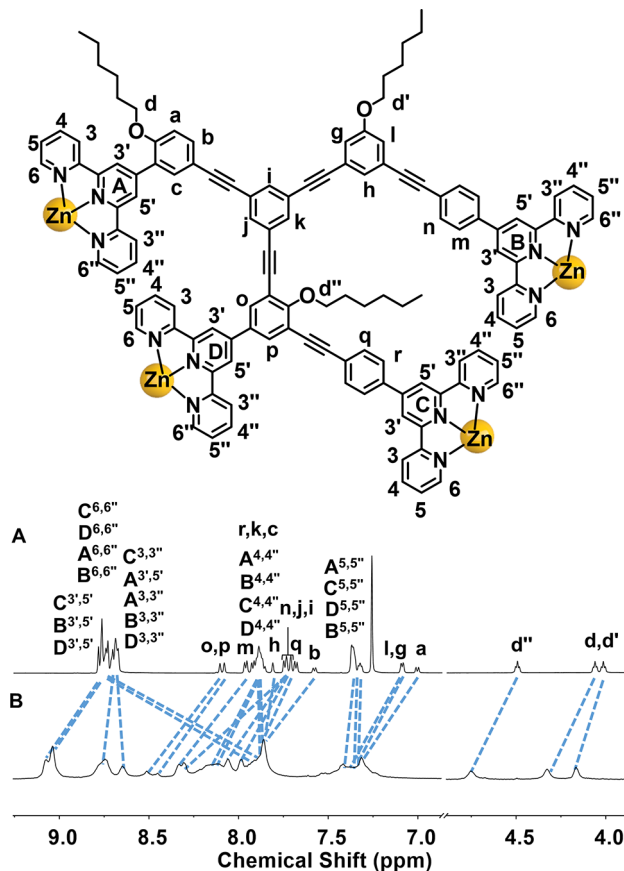


Figure 1. ^1H NMR spectra (600 MHz) of (A) ligand LA in CDCl_3 and (B) complexes A in CD_3CN .

As shown by 2D-COSY and NOESY results (Figures S99 and S101), four sets of proton signals from four different tpy units in the aromatic region can be distinguished. Compared with ligand LA, the signals of tpy^{A,B,C,D}- $H^{6,6''}$ protons showed a significant upfield shift ($\Delta\delta \approx 0.9$ ppm) on account of the electronic shielding effect,^{10a} indicating the coordination of tpy units with Zn(II). Meanwhile, all of the tpy- $H^{3',5'}$ protons exhibited a diagnostic downfield ($\Delta\delta \approx 0.3$ ppm) shift. The $-\text{OCH}_2-$ peaks of three alkyl chains ($-\text{OC}_6\text{H}_{13}$) at 4.75, 4.32, and 4.16 ppm were assigned to alkyl- $H^{d''}$, alkyl- $H^{d'}$, and alkyl- H^d , with an integration ratio of 1:1:1. Note that although multiple isomers existed simultaneously, the diffusion ordered spectroscopy

(DOSY) NMR spectrum of A (Figure S102) only displayed a narrow band at $\log D = -9.72$, perhaps owing to the similar sizes and shapes of the isomers and the limits of instrument resolution. The experimental diameter of A was calculated as ca. 6.5 nm using the modified Stokes-Einstein equation,²⁴ which agrees well with the theoretical prediction given by modeling structures.

ESI-MS and TWIM-MS have emerged as effective methods for analyzing the compositions and shapes of supramolecules.^{24,25} From the ESI-MS spectrum, one dominant set of peaks with charge states from 16+ to 24+ was observed (Figure 2A), resulting from successive loss of the counterions (PF_6^-).

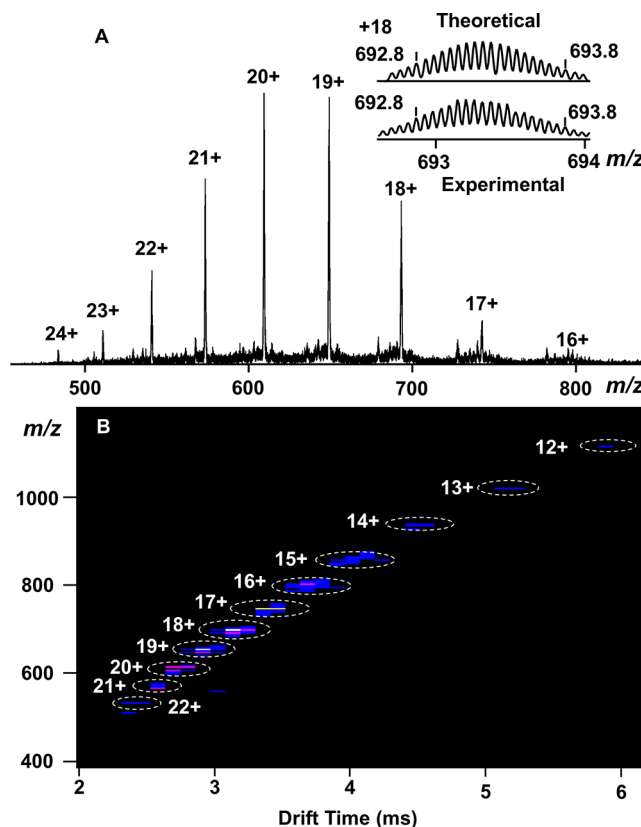


Figure 2. (A) ESI-MS and (B) TWIM-MS plot (m/z vs drift time) of complexes A. The charge states of intact assemblies are marked.

Further investigation revealed that each isotope pattern of these peaks matched well with the corresponding simulated isotope pattern of A with a molecular weight of 15 063.06 Da (Figure 2A and Figure S104). With four possible isomers in the system, the TWIM-MS spectrum (Figure 2B), however, exhibited only one narrow drift time distribution for each charge state, possibly on account of slight structural differences between four isomers and the resolution limits of the instrument.

Characterization of Complexes A by STM and Theoretical Study by DFT Calculations. To further investigate the structure of each isomer, high-resolution, ultrahigh-vacuum, low-temperature scanning tunneling microscopy (UHV-LT-STM) was utilized to explore the possible supramolecular isomers. The supramolecules were dissolved in CH_3CN and simply deposited on the surface of Ag(111) by drop-casting. Due to the octahedral coordination structure and high electron density, (tpy-Zn(II)-tpy) units give rise to a relatively strong signal in the form of a bright dot when

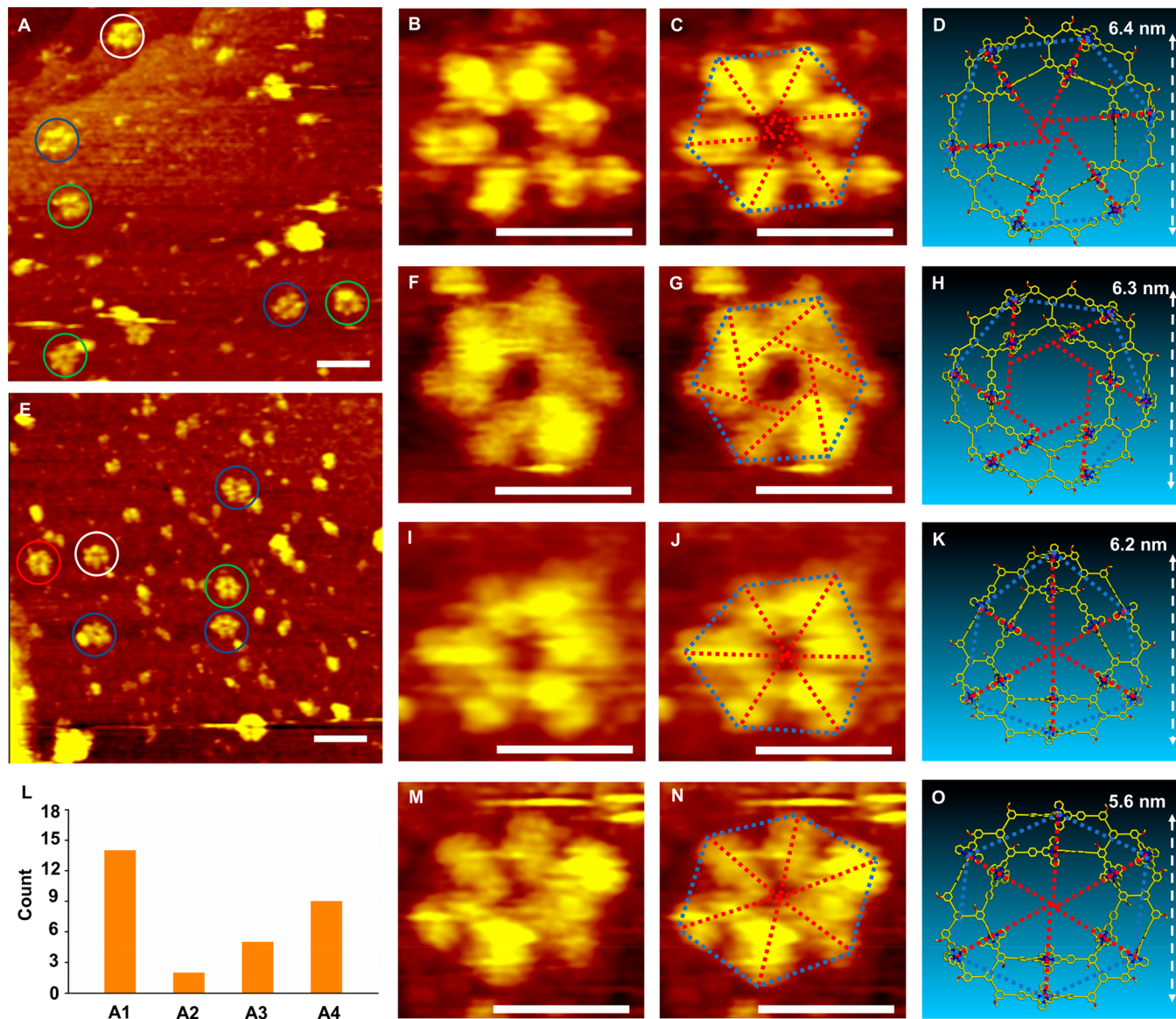


Figure 3. (A, E) STM imaging of complexes A on the Ag (111) surface with a scale bar of 10 nm (green circle, A1; red circle, A2; white circle, A3; blue circle, A4). (B, F, I, M) Enlarged STM images of complexes A1–A4 on the Ag (111) surface with a scale bar of 5 nm. (C, G, J, N) STM images of highlighted circles coordination sites of complexes A1–A4 with a scale bar of 5 nm. (D, H, K, O) Representative energy-minimized structures from molecular modeling of complexes A1–A4; alkyl chains were replaced by methoxy for clarity. (L) Distribution of four isomers based on the STM image for complexes A.

compared with the case of intramolecular organic fragments.^{23,26} On account of the short distance between the two layers, the signals of two adjacent $\langle\text{tpy-Zn(II)-tpy}\rangle$ units within different layers were merged and formed the oval-shaped lobes. By further investigating the direction, patterns, and geometries of the bright lobes, as expected, four types of isomers were observed from STM images (Figure 3 and Figures S154–S156). As illustrated by the distribution of $\langle\text{tpy-Zn(II)-tpy}\rangle$ junctions, each type of isomer can be differentiated from others. In order to confirm the shape and geometry of each isomer, dotted lines were added for the detailed patterns of supramolecules (Figure 3 and Figure S154). The orientations of adjacent inner and outer metal ions on the same side are shown as red lines, and the blue lines link the outer margin of metal ions and depict the shape of coordination site patterns. Thus, by measuring the angles between the red lines and blue lines, four isomers can be distinguished objectively (Figures S155–S158).

Regarding the symmetry of isomers' structures, A1 is centrosymmetric, but A3 is axisymmetric. It is worth noting that the subtle differences of distribution of $\langle\text{tpy-Zn(II)-tpy}\rangle$ junctions from A1 and A3 can be distinguished from STM imaging. STM imaging of supramolecules revealed clear images of circular structures with diameters at ca. 6.5 nm (Figure 3B,F,I,M), which is consistent with the energy-minimized structures from molecular modeling (Figure 3D,H,K,O). In addition, the statistical data of each isomer (Figure 3L and Figures S159–S161) indicated that the isomer of A1 has the largest abundance (47%), followed by isomers A4 (30%), A3 (16%), and A2 (7%).

To gain further insights about the distribution of isomers during the self-assembly of complexes A, total binding (intermolecular interaction) energy was used to compare the stabilities of different isomers by DFT simulation. During the self-assembly of complexes A, four isomers were assembled

because of the coexistence of two conformers of LA corresponding to four binding modes (Figure S153A). Given the large sizes of metallo-supramolecular isomers, we first calculated the binding energy of each binding mode in order to simplify the DFT calculation. Then, the total binding energy of each isomer was estimated as the sum of individual binding energies of six binding units within one structure. As shown in Table S1, isomer A1 ($E_{A1} = -787.253\ 623\ 2$ Hartree) exhibited the highest binding energy, followed by A4 ($E_{A4} = -787.247\ 005\ 8$ Hartree), A3 ($E_{A3} = -787.243\ 697\ 1$ Hartree), and A2 ($E_{A2} = -787.240\ 279\ 8$ Hartree). The order of total binding energies (A1 > A4 > A3 > A2) of four isomers is consistent with the order of experimental distribution of each isomer collected by STM imaging (Figure 3L), suggesting that the most abundant isomer A1 could be the most stable one with the highest binding energy.

Synthesis and Self-Assembly of Complexes B with One Binding Mode Followed by NMR and Mass Spectrometry Characterization. During the self-assembly of complexes A, four types of binding modes corresponding to two conformations of LA coexisted and resulted in four hexameric isomers. To further control the self-assembly of the dissymmetrical building block, another compact ligand LB was designed by shortening the linker between two layers and the length of two arms. Through such a design, we aimed to control the self-assembly of LB with one conformation by introducing steric hindrance, which could result in one binding mode as shown in Scheme 2B. Briefly, LB was obtained by the combination of Sonogashira and Suzuki coupling reactions. It was purified through a similar procedure as LA. Precursors and LB were fully characterized by ^1H , ^{13}C , 2D COSY, 2D NOESY, ESI-MS, and MALDI-TOF mass spectrometry.

The supramolecules were successfully prepared via the same self-assembly procedure as for complexes A. The formation of supramolecules was first characterized by ^1H NMR, 2D COSY, and NOESY NMR (Figures S143–S145). The ^1H NMR spectrum of assemblies shows four sets of tpy signals (Figure S148). Similar characteristic upfield shifts of tpy- $H^{6,6''}$ ($\Delta\delta \approx 0.98$ ppm) and downfield shifts of tpy- $H^{3',5'}$ ($\Delta\delta \approx 0.4$ ppm) were observed, indicating the coordination with Zn(II). The $-\text{OCH}_2-$ of three alkyl chains ($-\text{OC}_6\text{H}_{13}$) showed peaks at 4.38, 4.34, and 4.25 ppm, which correspond to alkyl- H^d , alkyl- $H^{d'}$, and alkyl- $H^{d''}$, with an integration ratio 1:1:1. DOSY NMR spectroscopy (Figure S146) showed a broad diffusion coefficient ($\log D = -9.69$ to -9.74) for all the relevant peaks, suggesting the existence of a mixture. As such, the supramolecular assembly of LB could differ from the result of LA, due to the different assembly behavior.

In ESI-MS and TWIM-MS spectra, three dominant complexes (hexagon, heptagon, and octagon) were detected in the system (Scheme 2), indicating that the compact structure of LB indeed altered the self-assembly process. Briefly, the ESI-MS spectrum showed three dominant sets of peaks with continuous charge states from 10+ to 22+ (Figure 4A). The isotope patterns of these peaks matched well with the corresponding simulated isotope patterns of hexamer $\text{Zn}_{12}\text{LB}_6$ (B1), heptamer $\text{Zn}_{14}\text{LB}_7$ (B2), and octamer $\text{Zn}_{16}\text{LB}_8$ (B3) with molecular weights of 14 631.06 Da, 17 069.57, and 19 505.08 Da (Figures S149–S151), respectively. Due to the apparent size difference of the hexamer, heptamer, and octamer, different charge states of the hexagon, heptagon, and octagon with a narrow time distribution were distinguished by TWIM-MS (Figure 4B). Given that four isomers were identified during the

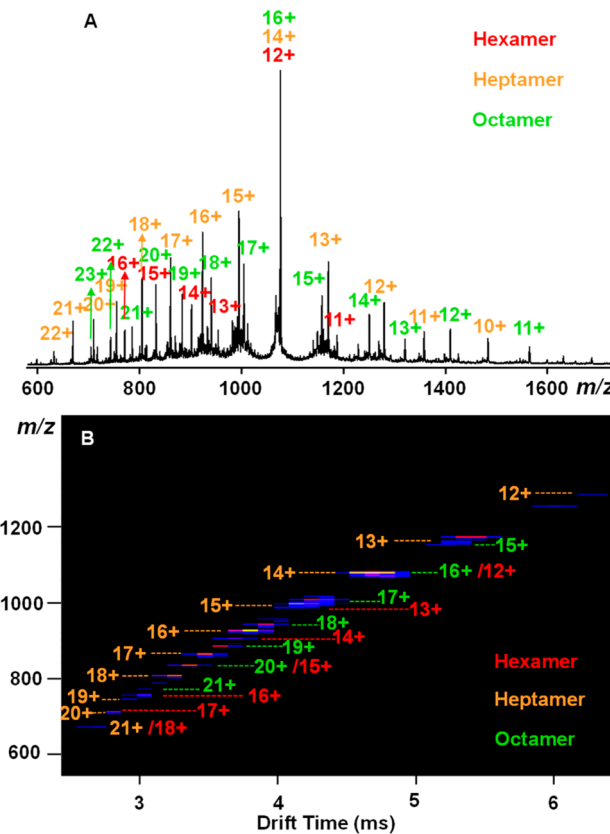


Figure 4. (A) ESI-MS and (B) 2D ESI-TWIM-MS plot (m/z vs drift time) of complexes B or $\text{Zn}_{2x}\text{LB}_x$ ($x = 6, 7, 8$). The charge states of the intact assemblies are marked.

assembly between Zn(II) and LA, the characterization of detailed structures for complexes B using STM turned out to be necessary.

Characterization of Complexes B by STM. From the STM images, hexamer, heptamer, and octamer were detected (Figure 5 and Figures S162–S164) as observed by ESI-MS. On account of the closer distance, the signals from two adjacent $\langle \text{tpy-Zn(II)-tpy} \rangle$ units have further merged into a circular lobe. The sizes of supramolecules measured by STM agreed well with the simulated structural sizes (Figure 5C,F,I). As shown by the distribution of three isomers imaged by STM (Figure S165), heptamer B2 is the foremost product (63.2%), followed by the octamer (28%) and hexamer (8.8%). The highest population of the heptamer further indicated the existence of substantial steric hindrance in the cyclic structures and expanded the angles between ligand arms to form larger rings. Interestingly, in comparison with the four binding modes during the self-assembly of LA with two major conformations, only one type of conformation corresponding to a single type of binding mode was found for the self-assembly of LB, which can be validated by the uniform distribution in the STM image (Figure 5). The average distribution of bright spots in Figure 5 indicated that the short and long arms of the inner and outer layers are staggered in the self-assembly process on account of the bulky size of $\langle \text{tpy-Zn(II)-tpy} \rangle$ junctions and steric hindrance between them. STM images also indicated that only spiral structures were generated in the $\text{Zn}_{2x}\text{LB}_x$ ($x = 6, 7, 8$) system. Therefore, by shortening the linkers between two layers and length of arms to introduce steric hindrance, the self-assembly behavior and conformations of

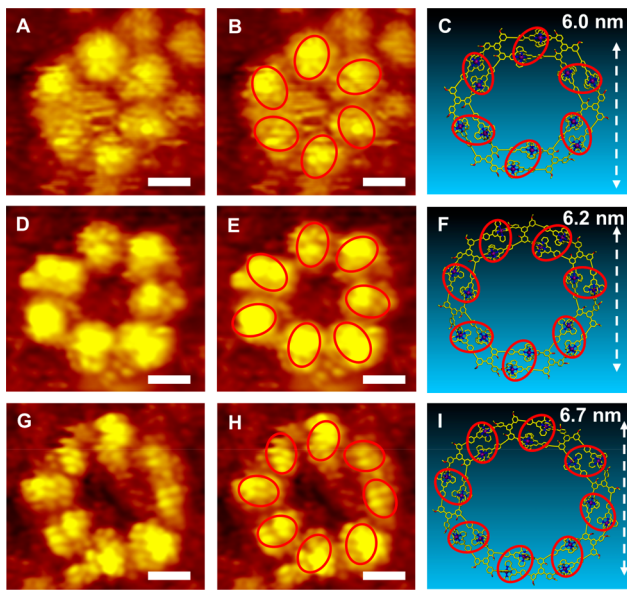


Figure 5. (A, D, G) STM imaging of the complexes B on the Ag (111) surface with a scale bar of 2 nm. (B, E, H) STM images of the highlighted circles showing the coordination site of complexes B1–B3. (C, F, I) Representative energy-minimized structures from molecular modeling of complexes B1–B3; alkyl chains were replaced by methoxy.

dissymmetrical building blocks of supramolecules could be further controlled.

Transmission Electron Microscopy (TEM) Characterization and Hierarchical Self-Assembly. Transmission electron microscopy (TEM) experiments were also performed to reveal the shapes and sizes of complexes A and B by deposition of dilute CH₃CN solutions ($\sim 10^{-6}$ M) on the surface of ultrathin carbon lacey support films on a copper grid. The reasonably measured dimensions were observed for both complexes A and B from TEM images (Figure 6A,E). The zoomed-in TEM images (Figure 6B,F) showed ringlike structures with hollow centers.

With the different assembled structures in hand, the hierarchical self-assembly behaviors of supramolecules A and B with long alkyl chains in different solvents were investigated. All the samples are obtained by diffusing diethyl ether into the solution of the complex (4 mg/mL in DMF). In Figure 6C, we observed that A could further self-assemble in nanotube structures, which were bound together to form fiberlike aggregates. The diameter (ca. 6.5 nm) of some nanotubes (Figure 6D) was consistent with that of individual supramolecules A from the energy-minimized structure. The hierarchical self-assembly result of nanofiber structures was likely attributed to multiple intermolecular interactions, such as π – π stacking, and CH– π hydrophobic/hydrophilic interactions.²⁷ Due to the existence of isomers with similar size, it is hard to recognize the molecular structures within fibers. Different with the hierarchical self-assembly behavior of A, spherical aggregates with diameters of about 50–250 nm were observed in the B system (Figure 6G,H). The different hierarchical self-assembly behaviors could be attributed to the following two aspects: (i) the reduced distance between inner and outer layers inhibits π – π stacking owing to the pseudo-octahedral configuration of tpy with transition metal ions; and (ii) the interior angles of heptamer and octamer are different from the designed 120° on the backbone, which may lead to

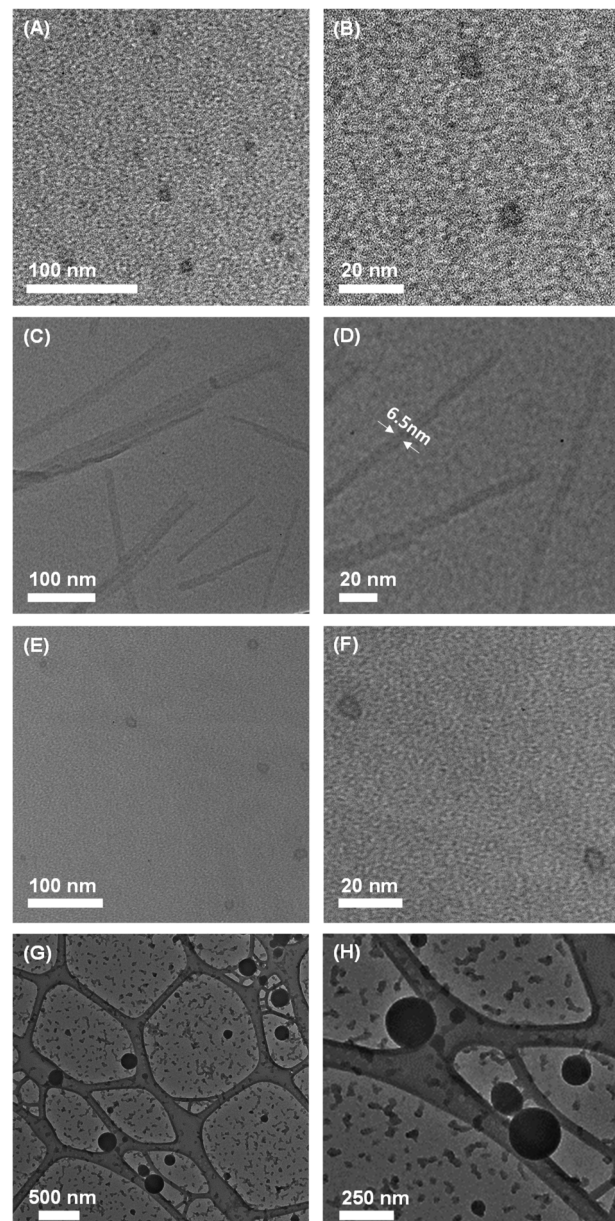


Figure 6. (A, E) TEM image of complexes A and B with a scale bar of 100 nm. (B, F) Enlarged TEM image of A and B with a scale bar of 20 nm. (C) TEM images of nanofiber structures formed by A with a scale bar of 100 nm. (D) Enlarged TEM images of nanofiber structures formed by A with a scale bar of 20 nm. (G) TEM images of spherical aggregates of B with a scale bar of 500 nm. (H) TEM images of spherical aggregates of B with a scale bar of 250 nm.

nonplanar structures and which hampered the hierarchical packing.

CONCLUSION

In summary, two novel supramolecular systems were successfully assembled through the coordination between dissymmetrical double-layered tetratopic 2,2':6',2''-terpyridine ligands and Zn(II). In addition to the conventional characterization techniques (including NMR, MS, and TEM), UHV-LT-STM was utilized to investigate the structures of isomeric systems at the submolecular level. The STM statistical data and DFT calculation revealed that four hexameric isomers existed in the self-assembly of supramolecules A because of the four types of

binding modes during the self-assembly of ligand **LA** with two major conformations. Among all isomers, **A1** had the highest total binding energy in the DFT calculation and the highest abundance in STM imaging statistical results. Different from the self-assembly of supramolecules **A**, the hexamer, heptamer, and octamer were generated in the self-assembly of supramolecules **B** with composition $Zn_{2x}LB_x$ ($x = 6, 7$, and 8). STM images further revealed that only a single conformation corresponding to one binding mode was found for ligand **LB**. Among these spiral structures, the heptamer was the foremost product followed by the octamer and hexamer. As such, the self-assembly behavior and structures of supramolecules could be controlled by adjusting the length of arms and the distance of two layers. This work offered a promising avenue for the design and characterization of supramolecular architectures with dissymmetrical ligands and sheds light on the insight of coordination-driven self-assembly processes.

■ ASSOCIATED CONTENT

SI Supporting Information

The Supporting Information is available free of charge at <https://pubs.acs.org/doi/10.1021/jacs.0c12508>.

Synthetic details and characterizations of ligands and complexes including NMR, ESI-MS, TWIM-MS, DFT calculation, and STM ([PDF](#))

■ AUTHOR INFORMATION

Corresponding Authors

Ming Wang – State Key Laboratory of Supramolecular Structure and Materials, College of Chemistry, Jilin University, Changchun, Jilin 130012, China; [ORCID.org/0000-0002-5332-0804](#); Email: mingwang358@jlu.edu.cn

Xiaopeng Li – College of Chemistry and Environmental Engineering and Shenzhen University General Hospital, Clinical Medical Academy, Shenzhen University, Shenzhen, Guangdong 518055, China; [ORCID.org/0000-0001-9655-9551](#); Email: xiaopengli@szu.edu.cn

Authors

Junjuan Shi – State Key Laboratory of Supramolecular Structure and Materials, College of Chemistry, Jilin University, Changchun, Jilin 130012, China; College of Chemistry and Environmental Engineering, Shenzhen University, Shenzhen, Guangdong 518055, China

Yiming Li – College of Chemistry and Environmental Engineering, Shenzhen University, Shenzhen, Guangdong 518055, China; Department of Chemistry, University of South Florida, Tampa, Florida 33620, United States

Xin Jiang – State Key Laboratory of Supramolecular Structure and Materials, College of Chemistry, Jilin University, Changchun, Jilin 130012, China

Hao Yu – State Key Laboratory of Supramolecular Structure and Materials, College of Chemistry, Jilin University, Changchun, Jilin 130012, China

Jiaqi Li – State Key Laboratory of Supramolecular Structure and Materials, College of Chemistry, Jilin University, Changchun, Jilin 130012, China

Houyu Zhang – State Key Laboratory of Supramolecular Structure and Materials, College of Chemistry, Jilin University, Changchun, Jilin 130012, China; [ORCID.org/0000-0003-0360-6035](#)

Daniel J. Trainer – Nanoscience and Technology Division, Argonne National Laboratory, Lemont, Illinois 60439, United States

Saw Wai Hla – Nanoscience and Technology Division, Argonne National Laboratory, Lemont, Illinois 60439, United States

Heng Wang – College of Chemistry and Environmental Engineering, Shenzhen University, Shenzhen, Guangdong 518055, China

Complete contact information is available at:

<https://pubs.acs.org/10.1021/jacs.0c12508>

Author Contributions

[#]J.S. and Y.L. contributed equally.

Notes

The authors declare no competing financial interest.

■ ACKNOWLEDGMENTS

We gratefully acknowledge the support from the National Natural Science Foundation of China (22071079 for M.W.) and mass spectrometry characterization by Molecular Scale Laboratories. X.L. acknowledges the support from Tencent Founders Alumni Foundation.

■ REFERENCES

- (1) (a) Cram, D. J. The Design of Molecular Hosts, Guests, and Their Complexes. *Angew. Chem., Int. Ed. Engl.* **1988**, *27* (8), 1009–1020. (b) Pedersen, C. J. The Discovery of Crown Ethers. *Angew. Chem., Int. Ed. Engl.* **1988**, *27* (8), 1021–1027. (c) Lehn, J.-M. Supramolecular Chemistry—Scope and Perspectives Molecules, Supermolecules, and Molecular Devices. *Angew. Chem., Int. Ed. Engl.* **1988**, *27* (1), 89–112.
- (2) (a) Philp, D.; Stoddart, J. F. Self-Assembly in Natural and Unnatural Systems. *Angew. Chem., Int. Ed. Engl.* **1996**, *35* (11), 1154–1196. (b) Forgan, R. S.; Sauvage, J.-P.; Stoddart, J. F. Chemical Topology: Complex Molecular Knots, Links, and Entanglements. *Chem. Rev.* **2011**, *111* (9), 5434–5464. (c) Hargrove, A. E.; Nieto, S.; Zhang, T.; Sessler, J. L.; Anslyn, E. V. Artificial Receptors for the Recognition of Phosphorylated Molecules. *Chem. Rev.* **2011**, *111* (11), 6603–6782.
- (3) (a) Caulder, D. L.; Raymond, K. N. Supermolecules by Design. *Acc. Chem. Res.* **1999**, *32* (11), 975–982. (b) Hofmeier, H.; Schubert, U. S. Recent Developments in the Supramolecular Chemistry of Terpyridine-Metal Complexes. *Chem. Soc. Rev.* **2004**, *33* (6), 373–399. (c) Wild, A.; Winter, A.; Schlüter, F.; Schubert, U. S. Advances in the Field of π -Conjugated 2,2':6',2"-Terpyridines. *Chem. Soc. Rev.* **2011**, *40* (3), 1459–1511.
- (4) (a) Würthner, F.; You, C.-C.; Saha-Möller, C. R. Metallosupramolecular Squares: From Structure to Function. *Chem. Soc. Rev.* **2004**, *33* (3), 133–146. (b) Meyer, C. D.; Joiner, C. S.; Stoddart, J. F. Template-Directed Synthesis Employing Reversible Imine Bond Formation. *Chem. Soc. Rev.* **2007**, *36* (11), 1705–1723. (c) Chakraborty, R.; Mukherjee, P. S.; Stang, P. J. Supramolecular Coordination: Self-Assembly of Finite Two- and Three-Dimensional Ensembles. *Chem. Rev.* **2011**, *111* (11), 6810–6918. (d) Han, M.; Engelhard, D. M.; Clever, G. H. Self-Assembled Coordination Cages Based on Banana-Shaped Ligands. *Chem. Soc. Rev.* **2014**, *43* (6), 1848–1860. (e) Cook, T. R.; Stang, P. J. Recent Developments in the Preparation and Chemistry of Metallacycles and Metallacages via Coordination. *Chem. Rev.* **2015**, *115* (15), 7001–7045. (f) Newkome, G. R.; Moorefield, C. N. From 1→3 Dendritic Designs to Fractal Supramolecular Constructs: Understanding the Pathway to the Sierpinski Gasket. *Chem. Soc. Rev.* **2015**, *44* (12), 3954–3967. (g) Chen, L.-J.; Yang, H.-B.; Shionoya, M. Chiral Metallosupramolecular Architectures. *Chem. Soc. Rev.* **2017**, *46* (9), 2555–2576. (h) Chakraborty, S.; Newkome, G. R. Terpyridine-Based Metallosupramolecular Constructs: Tailored Monomers to Precise 2D-Motifs and 3D-Metallocages. *Chem. Soc. Rev.* **2018**, *47* (11), 3991–

4016. (i) Pan, M.; Wu, K.; Zhang, J.-H.; Su, C.-Y. Chiral Metal-Organic Cages/Containers (MOCs): From Structural and Stereochemical Design to Applications. *Coord. Chem. Rev.* **2019**, *378*, 333–349. (j) Wang, W.; Wang, Y.-X.; Yang, H.-B. Supramolecular Transformations within Discrete Coordination-Driven Supramolecular Architectures. *Chem. Soc. Rev.* **2016**, *45* (9), 2656–2693. (k) Gao, W.-X.; Feng, H.-J.; Guo, B.-B.; Lu, Y.; Jin, G.-X. Coordination-Directed Construction of Molecular Links. *Chem. Rev.* **2020**, *120* (13), 6288–6325. (l) Jin, Y.; Zhang, Q.; Zhang, Y.; Duan, C. Electron Transfer in the Confined Environments of Metal-Organic Coordination Supramolecular Systems. *Chem. Soc. Rev.* **2020**, *49* (15), 5561–5600. (m) Sun, Y.; Chen, C.; Liu, J.; Stang, P. J. Recent developments in the construction and applications of platinum-based metallacycles and metallacages via coordination. *Chem. Soc. Rev.* **2020**, *49* (12), 3889–3919.
- (5) (a) Stang, P. J.; Olenyuk, B. Self-Assembly, Symmetry, and Molecular Architecture: Coordination as the Motif in the Rational Design of Supramolecular Metallacyclic Polygons and Polyhedra. *Acc. Chem. Res.* **1997**, *30* (12), 502–518. (b) Seidel, S. R.; Stang, P. J. High-Symmetry Coordination Cages via Self-Assembly. *Acc. Chem. Res.* **2002**, *35* (11), 972–983. (c) Fujita, M.; Tominaga, M.; Hori, A.; Therrien, B. Coordination Assemblies from a Pd(II)-Cornered Square Complex. *Acc. Chem. Res.* **2005**, *38* (4), 369–378. (d) Nitschke, J. R. Construction, Substitution, and Sorting of Metallo-Organic Structures via Subcomponent Self-Assembly. *Acc. Chem. Res.* **2007**, *40* (2), 103–112. (e) Castilla, A. M.; Ramsay, W. J.; Nitschke, J. R. Stereochemistry in Subcomponent Self-Assembly. *Acc. Chem. Res.* **2014**, *47* (7), 2063–2073. (f) Jansze, S. M.; Severin, K. Clathrochelate Metalloligands in Supramolecular Chemistry and Materials Science. *Acc. Chem. Res.* **2018**, *51* (9), 2139–2147.
- (6) (a) Holliday, B. J.; Mirkin, C. A. Strategies for the Construction of Supramolecular Compounds through Coordination Chemistry. *Angew. Chem., Int. Ed.* **2001**, *40* (11), 2022–2043. (b) Sepehpour, H.; Fu, W.; Sun, Y.; Stang, P. J. Biomedically Relevant Self-Assembled Metallacycles and Metallacages. *J. Am. Chem. Soc.* **2019**, *141* (36), 14005–14020.
- (7) (a) Schweiger, M.; Seidel, S. R.; Arif, A. M.; Stang, P. J. The Self-Assembly of an Unexpected, Unique Supramolecular Triangle Composed of Rigid Subunits. *Angew. Chem., Int. Ed.* **2001**, *40* (18), 3467–3469. (b) Kryschko, Y. K.; Seidel, S. R.; Arif, A. M.; Stang, P. J. Coordination-Driven Self-Assembly of Predesigned Supramolecular Triangles. *J. Am. Chem. Soc.* **2003**, *125* (17), 5193–5198. (c) Heo, J.; Jeon, Y.-M.; Mirkin, C. A. Reversible Interconversion of Homochiral Triangular Macrocycles and Helical Coordination Polymers. *J. Am. Chem. Soc.* **2007**, *129* (25), 7712–7713. (d) Zangrandi, E.; Casanova, M.; Alessio, E. Trinuclear Metallacycles: Metallatriangles and Much More. *Chem. Rev.* **2008**, *108* (12), 4979–5013. (e) Schmittel, M.; Mahata, K. A Fully Dynamic Five-Component Triangle via Self-Sorting. *Chem. Commun.* **2010**, *46* (23), 4163–4165. (f) Liu, Z.; Liu, G.; Wu, Y.; Cao, D.; Sun, J.; Schneebeli, S. T.; Nassar, M. S.; Mirkin, C. A.; Stoddart, J. F. Assembly of Supramolecular Nanotubes from Molecular Triangles and 1,2-Dihalohydrocarbons. *J. Am. Chem. Soc.* **2014**, *136* (47), 16651–16660. (g) Wood, D. M.; Meng, W. J.; Ronson, T. K.; Stefankiewicz, A. R.; Sanders, J. K. M.; Nitschke, J. R. Guest-Induced Transformation of a Porphyrin-Edged Fe^{II}₄L₆ Capsule into a Cu^IFe^{II}₂L₄ Fullerene Receptor. *Angew. Chem., Int. Ed.* **2015**, *54* (13), 3988–3992.
- (8) (a) Fujita, M.; Yazaki, J.; Ogura, K. Preparation of a Macroyclic Polynuclear Complex, [(en)Pd(4,4'-Bpy)]₄(NO₃)₈¹⁻ Which Recognizes an Organic Molecule in Aqueous Media. *J. Am. Chem. Soc.* **1990**, *112* (14), 5645–5647. (b) Stang, P. J.; Cao, D. H. Transition Metal Based Cationic Molecular Boxes. Self-Assembly of Macroyclic Platinum(II) and Palladium(II) Tetranuclear Complexes. *J. Am. Chem. Soc.* **1994**, *116* (11), 4981–4982. (c) Stang, P. J.; Cao, D. H.; Saito, S.; Arif, A. M. Self-Assembly of Cationic, Tetranuclear, Pt(II) and Pd(II) Macroyclic Squares. X-Ray Crystal Structure of [Pt²⁺(dppp)-(4,4'-bipyridyl)2-OSO₂CF₃]₄. *J. Am. Chem. Soc.* **1995**, *117* (23), 6273–6283. (d) Fujita, M.; Sasaki, O.; Mitsuhashi, T.; Fujita, T.; Yazaki, J.; Yamaguchi, K.; Ogura, K. On the Structure of Transition-Metal-Linked Molecular Squares. *Chem. Commun.* **1996**, 1535–1536. (e) Olenyuk, B.; Whiteford, J. A.; Stang, P. J. Design and Study of Synthetic Chiral Nanoscopic Assemblies. Preparation and Characterization of Optically Active Hybrid, Iodonium-Transition-Metal and All-Transition-Metal Macrocyclic Molecular Squares. *J. Am. Chem. Soc.* **1996**, *118* (35), 8221–8230. (f) Stang, P. J.; Olenyuk, B. Directed Self-Assembly of Chiral, Optically Active Macrocyclic Tetranuclear Molecular Squares. *Angew. Chem., Int. Ed. Engl.* **1996**, *35* (7), 732–736.
- (9) (a) Perera, S.; Li, X.; Soler, M.; Schultz, A.; Wesdemiotis, C.; Moorefield, C. N.; Newkome, G. R. Hexameric Palladium(II) Terpyridyl Metallamacrocycles: Assembly with 4,4'-Bipyridine and Characterization by TWIM Mass Spectrometry. *Angew. Chem., Int. Ed.* **2010**, *49* (37), 6539–6544. (b) Wang, M.; Wang, C.; Hao, X.-Q.; Liu, J.; Li, X.; Xu, C.; Lopez, A.; Sun, L.; Song, M.-P.; Yang, H.-B.; Li, X. Hexagon Wreaths: Self-Assembly of Discrete Supramolecular Fractal Architectures Using Multitopic Terpyridine Ligands. *J. Am. Chem. Soc.* **2014**, *136* (18), 6664–6671. (c) Li, Y.; Jiang, Z.; Wang, M.; Yuan, J.; Liu, D.; Yang, X.; Chen, M.; Yan, J.; Li, X.; Wang, P. Giant, Hollow 2D Metallocarchitecture: Stepwise Self-Assembly of a Hexagonal Supramolecular Nut. *J. Am. Chem. Soc.* **2016**, *138* (31), 10041–10046. (d) Yan, X. Z.; Wang, M.; Cook, T. R.; Zhang, M. M.; Saha, M. L.; Zhou, Z. X.; Li, X. P.; Huang, F. H.; Stang, P. J. Light-Emitting Superstructures with Anion Effect: Coordination-Driven Self-Assembly of Pure Tetraphenylethylene Metallacycles and Metallacages. *J. Am. Chem. Soc.* **2016**, *138* (13), 4580–4588. (e) Wang, M.; Wang, K.; Wang, C.; Huang, M.; Hao, X.-Q.; Shen, M.-Z.; Shi, G. Q.; Zhang, Z.; Song, B.; Cisneros, A.; Song, M.-P.; Xu, B.; Li, X. Self-Assembly of Concentric Hexagons and Hierarchical Self-Assembly of Supramolecular Metal-Organic Nanoribbons at the Solid/Liquid Interface. *J. Am. Chem. Soc.* **2016**, *138* (29), 9258–9268.
- (10) (a) Wang, J.-L.; Li, X.; Lu, X.; Hsieh, I.-F.; Cao, Y.; Moorefield, C. N.; Wesdemiotis, C.; Cheng, S. Z.; Newkome, G. R. Stoichiometric Self-Assembly of Shape-Persistent 2D Complexes: A Facile Route to a Symmetric Supramacromolecular Spoked Wheel. *J. Am. Chem. Soc.* **2011**, *133* (30), 11450–11453. (b) Lu, X.; Li, X.; Cao, Y.; Schultz, A.; Wang, J.-L.; Moorefield, C. N.; Wesdemiotis, C.; Cheng, S. Z.; Newkome, G. R. Self-Assembly of a Supramolecular, Three-Dimensional, Spoked, Bicycle-Like Wheel. *Angew. Chem., Int. Ed.* **2013**, *52* (30), 7728–7731. (c) Lu, X.; Li, X.; Guo, K.; Wang, J.; Huang, M.; Wang, J.-L.; Xie, T.-Z.; Moorefield, C. N.; Cheng, S. Z.; Wesdemiotis, C.; Newkome, G. R. One Ligand in Dual Roles: Self-Assembly of a Bis-Rhombohedral-Shaped, Three-Dimensional Molecular Wheel. *Chem. - Eur. J.* **2014**, *20* (41), 13094–13098.
- (11) (a) Toyota, S.; Woods, C. R.; Benaglia, M.; Haldimann, R.; Wärnmark, K.; Hardcastle, K.; Siegel, J. S. Tetranuclear Copper(I)-Biphenanthroline Gridwork: Violation of the Principle of Maximal Donor Coordination Caused by Intercalation and CH-to-N Forces. *Angew. Chem., Int. Ed.* **2001**, *40* (4), 751–754. (b) Schmittel, M.; Kalsani, V.; Fenske, D.; Wiegrafe, A. Self-Assembly of Heteroleptic [2 × 2] and [2 × 3] Nanogrids. *Chem. Commun.* **2004**, No. 5, 490–491. (c) Schmittel, M.; Kalsani, V.; Bats, J. W. Metal-Driven and Covalent Synthesis of Supramolecular Grids from Racks: A Convergent Approach to Heterometallic and Heteroleptic Nanostructures. *Inorg. Chem.* **2005**, *44* (12), 4115–4117. (d) Dhers, S.; Mondal, A.; Aguilà, D.; Ramirez, J.; Vela, S.; Dechambenoit, P.; Rouzieres, M.; Nitschke, J. R.; Clerac, R.; Lehn, J. M. Spin State Chemistry: Modulation of Ligand pK(a) by Spin State Switching in a [2 × 2] Iron(II) Grid-Type Complex. *J. Am. Chem. Soc.* **2018**, *140* (26), 8218–8227.
- (12) (a) Caulder, D. L.; Powers, R. E.; Parac, T. N.; Raymond, K. N. The Self-Assembly of a Predesigned Tetrahedral M₄L₆ Supramolecular Cluster. *Angew. Chem., Int. Ed.* **1998**, *37* (13–14), 1840–1843. (b) Mal, P.; Schultz, D.; Beyeh, K.; Rissanen, K.; Nitschke, J. R. An Unlockable-Relockable Iron Cage by Subcomponent Self-Assembly. *Angew. Chem., Int. Ed.* **2008**, *47* (43), 8297–8301. (c) Black, S. P.; Stefankiewicz, A. R.; Smulders, M. M. J.; Sattler, D.; Schalley, C. A.; Nitschke, J. R.; Sanders, J. K. M. Generation of a Dynamic System of Three-Dimensional Tetrahedral Polycatenanes. *Angew. Chem., Int. Ed.* **2013**, *52* (22), 5749–5752. (d) Ludlow, J. M., III; Xie, T.; Guo, Z.; Guo, K.; Saunders, M. J.; Moorefield, C. N.; Wesdemiotis, C.; Newkome, G. R. Directed Flexibility: Self-Assembly of a Supramolecular Tetrahedron.

- Chem. Commun.* **2015**, *51* (18), 3820–3823. (e) McConnell, A. J.; Aitchison, C. M.; Grommet, A. B.; Nitschke, J. R. Subcomponent Exchange Transforms an $\text{Fe}^{\text{II}}\text{L}_4$ Cage from High- to Low-Spin, Switching Guest Release in a Two-Cage System. *J. Am. Chem. Soc.* **2017**, *139* (18), 6294–6297. (f) Liu, D.; Chen, M.; Li, K.; Li, Z.; Huang, J.; Wang, J.; Jiang, Z.; Zhang, Z.; Xie, T.; Newkome, G. R.; Wang, P. Giant Truncated Metallo-Tetrahedron with Unexpected Supramolecular Aggregation Induced Emission Enhancement. *J. Am. Chem. Soc.* **2020**, *142* (17), 7987–7994.
- (13) (a) Olenyuk, B.; Whiteford, J. A.; Fechtenkötter, A.; Stang, P. J. Self-Assembly of Nanoscale Cuboctahedraby Coordination Chemistry. *Nature* **1999**, *398* (6730), 796–799. (b) Sun, Q.-F.; Sato, S.; Fujita, M. An $\text{M}_{18}\text{L}_{24}$ Stellated Cuboctahedron through Post-Stellation of an $\text{M}_{12}\text{L}_{24}$ Core. *Nat. Chem.* **2012**, *4* (4), 330–333. (c) Xie, T.-Z.; Guo, K.; Guo, Z.; Gao, W.-Y.; Wojtas, L.; Ning, G.-H.; Huang, M.; Lu, X.; Li, J.-Y.; Liao, S.-Y.; Chen, Y.-S.; Moorefield, C. N.; Saunders, M. J.; Cheng, S. Z.; Wesdemiotis, C.; Newkome, G. R. Precise Molecular Fission and Fusion: Quantitative Self-Assembly and Chemistry of a Metallo-Cuboctahedron. *Angew. Chem., Int. Ed.* **2015**, *54* (32), 9224–9229. (d) Xie, T.-Z.; Endres, K. J.; Guo, Z.; Ludlow, J. M., III; Moorefield, C. N.; Saunders, M. J.; Wesdemiotis, C.; Newkome, G. R. Controlled Interconversion of Superposed-Bistriangle, Octahedron, and Cuboctahedron Cages Constructed Using a Single, Terpyridinyl-Based Polyligand and Zn^{2+} . *J. Am. Chem. Soc.* **2016**, *138* (38), 12344–12347.
- (14) (a) Meng, W. J.; Breiner, B.; Rissanen, K.; Thoburn, J. D.; Clegg, J. K.; Nitschke, J. R. A Self-Assembled M_8L_6 Cubic Cage That Selectively Encapsulates Large Aromatic Guests. *Angew. Chem., Int. Ed.* **2011**, *50* (15), 3479–3483. (b) Ramsay, W. J.; Ronson, T. K.; Clegg, J. K.; Nitschke, J. R. Bidirectional Regulation of Halide Binding in a Heterometallic Supramolecular Cube. *Angew. Chem., Int. Ed.* **2013**, *52* (50), 13439–13443. (c) Ramsay, W. J.; Nitschke, J. R. Two Distinct Allosteric Active Sites Regulate Guest Binding within a $\text{Fe}_8\text{Mo}_{12}^{16+}$ Cubic Receptor. *J. Am. Chem. Soc.* **2014**, *136* (19), 7038–7043. (d) Wang, M.; Wang, C.; Hao, X.-Q.; Li, X.; Vaughn, T. J.; Zhang, Y.-Y.; Yu, Y.; Li, Z.-Y.; Song, M.-P.; Yang, H.-B.; Li, X. From Trigonal Bipyramidal to Platonic Solids: Self-Assembly and Self-Sorting Study of Terpyridine-Based 3D Architectures. *J. Am. Chem. Soc.* **2014**, *136* (29), 10499–10507. (e) Ramsay, W. J.; Szczypinski, F. T.; Weissman, H.; Ronson, T. K.; Smulders, M. M. J.; Rybtchinski, B.; Nitschke, J. R. Designed Enclosure Enables Guest Binding within the 4200 \AA^3 Cavity of a Self-Assembled Cube. *Angew. Chem., Int. Ed.* **2015**, *54* (19), 5636–5640. (f) Ramsay, W. J.; Rizzuto, F. J.; Ronson, T. K.; Caprice, K.; Nitschke, J. R. Subtle Ligand Modification Inverts Guest Binding Hierarchy in $\text{M}^{\text{II}}\text{L}_6$ Supramolecular Cubes. *J. Am. Chem. Soc.* **2016**, *138* (23), 7264–7267. (g) Mosquera, J.; Szyszko, B.; Ho, S. K. Y.; Nitschke, J. R. Sequence-Selective Encapsulation and Protection of Long Peptides by a Self-Assembled $\text{Fe}^{\text{II}}\text{L}_6$ Cubic Cage. *Nat. Commun.* **2017**, *8* (1), 14482. (h) Pilgrim, B. S.; Roberts, D. A.; Lohr, T. G.; Ronson, T. K.; Nitschke, J. R. Signal Transduction in a Covalent Post-Assembly Modification Cascade. *Nat. Chem.* **2017**, *9* (12), 1276–1281.
- (15) (a) Hiraoka, S.; Yamauchi, Y.; Arakane, R.; Shionoya, M. Template-Directed Synthesis of a Covalent Organic Capsule Based on a 3 nm-Sized Metallocapsule. *J. Am. Chem. Soc.* **2009**, *131* (33), 11646–11647. (b) He, L.; Wang, S.-C.; Lin, L.-T.; Cai, J.-Y.; Li, L.; Tu, T.-H.; Chan, Y.-T. Multicomponent Metallo-Supramolecular Nanocapsules Assembled from Calix[4]Resorcinarene-Based Terpyridine Ligands. *J. Am. Chem. Soc.* **2020**, *142* (15), 7134–7144.
- (16) (a) Lehn, J.-M.; Rigault, A.; Siegel, J.; Harrowfield, J.; Chevrier, B.; Moras, D. Spontaneous Assembly of Double-Stranded Helicates from Oligobipyridine Ligands and Copper(I) Cations: Structure of an Inorganic Double Helix. *Proc. Natl. Acad. Sci. U. S. A.* **1987**, *84* (9), 2565–2569. (b) Baxter, P.; Lehn, J.-M.; DeCian, A.; Fischer, J. Multicomponent Self-Assembly: Spontaneous Formation of a Cylindrical Complex from Five Ligands and Six Metal Ions. *Angew. Chem., Int. Ed. Engl.* **1993**, *32* (1), 69–72. (c) Hasenkopf, B.; Lehn, J.-M.; Boumediene, N.; Dupont-Gervais, A.; Dorselaer, A. V.; Kneisel, B.; Fenske, D. Self-Assembly of Tetra- and Hexanuclear Circular Helicates. *J. Am. Chem. Soc.* **1997**, *119* (45), 10956–10962.
- (17) (a) Barran, P. E.; Cole, H. L.; Goldup, S. M.; Leigh, D. A.; McGonigal, P. R.; Symes, M. D.; Wu, J.; Zengerle, M. Active-Metal Template Synthesis of a Molecular Trefoil Knot. *Angew. Chem., Int. Ed.* **2011**, *50* (51), 12280–12284. (b) Romuald, C.; Coutrot, F. Combining Coordination Chemistry and Catalysis to Tie a Knot by an Active-Metal Template Strategy. *Angew. Chem., Int. Ed.* **2012**, *51* (11), 2544–2545. (c) Leigh, D. A.; Pirvu, L.; Schaufelberger, F.; Tetlow, D. J.; Zhang, L. Securing a Supramolecular Architecture by Tying a Stopper Knot. *Angew. Chem., Int. Ed.* **2018**, *57* (33), 10484–10488.
- (18) (a) Sun, Q.-F.; Iwasa, J.; Ogawa, D.; Ishido, Y.; Sato, S.; Ozeki, T.; Sei, Y.; Yamaguchi, K.; Fujita, M. Self-Assembled $\text{M}_{24}\text{L}_{48}$ Polyhedra and Their Sharp Structural Switch Upon Subtle Ligand Variation. *Science* **2010**, *328* (5982), 1144–1147. (b) Bunzen, J.; Iwasa, J.; Bonakdarzadeh, P.; Numata, E.; Rissanen, K.; Sato, S.; Fujita, M. Self-Assembly of $\text{M}_{24}\text{L}_{48}$ Polyhedra Based on Empirical Prediction. *Angew. Chem., Int. Ed.* **2012**, *51* (13), 3161–3163. (c) Xie, T.-Z.; Liao, S.-Y.; Guo, K.; Lu, X.; Dong, X.; Huang, M.; Moorefield, C. N.; Cheng, S. Z.; Liu, X.; Wesdemiotis, C.; Newkome, G. R. Construction of a Highly Symmetric Nanosphere via a One-Pot Reaction of a Tristerpyridine Ligand with Ru(II). *J. Am. Chem. Soc.* **2014**, *136* (23), 8165–8168. (d) Wang, Q.-Q.; Gonell, S.; Leenders, S. H. A. M.; Dür, M.; Ivanović-Burmazović, I.; Reek, J. N. H. Self-Assembled Nanospheres with Multiple Endohedral Binding Sites Pre-Organize Catalysts and Substrates for Highly Efficient Reactions. *Nat. Chem.* **2016**, *8* (3), 225–230. (e) Chen, Y.-S.; Solei, E.; Huang, Y.-F.; Wang, C.-L.; Tu, T.-H.; Keinan, E.; Chan, Y.-T. Chemical Mimicry of Viral Capsid Self-Assembly via Corannulene-Based Pentatopic Tectons. *Nat. Commun.* **2019**, *10* (1), 3443.
- (19) (a) Doolittle, R. F. Proteins. *Sci. Am.* **1985**, *253*, 88–99. (b) Xu, Z.; Horwich, A. L.; Sigler, P. B. The Crystal Structure of the Asymmetric Groel-Groes-(Adp)₇ Chaperonin Complex. *Nature* **1997**, *388* (6644), 741–750. (c) Branden, Ivar, C.; Tooze, J. *Introduction to Protein Structure*; Garland Science, 2012.
- (20) (a) Qin, Z.; Jennings, M. C.; Puddephatt, R. J. Stacked Molecular Triangles: Self-Assembly Using Coordination Chemistry and Hydrogen Bonding. *Chem. Commun.* **2001**, *24*, 2676–2677. (b) Chi, K.-W.; Addicott, C.; Arif, A. M.; Stang, P. J. Ambidentate Pyridyl-Carboxylate Ligands in the Coordination-Driven Self-Assembly of 2D Pt Macrocycles: Self-Selection for a Single Isomer. *J. Am. Chem. Soc.* **2004**, *126* (50), 16569–16574. (c) Ghosh, S.; Mukherjee, P. S. Self-Assembly of Metal-Organic Hybrid Nanoscopic Rectangles. *Dalton Trans.* **2007**, 2542–2546. (d) Zhao, L.; Northrop, B. H.; Zheng, Y. R.; Yang, H. B.; Lee, H. J.; Lee, Y. M.; Park, J. Y.; Chi, K. W.; Stang, P. J. Self-Selection in the Self-Assembly of Isomeric Supramolecular Squares from Unsymmetrical Bis(4-Pyridyl)Acetylene Ligands. *J. Org. Chem.* **2008**, *73* (17), 6580–6586. (e) Zheng, Y.-R.; Northrop, B. H.; Yang, H.-B.; Zhao, L.; Stang, P. J. Geometry Directed Self-Selection in the Coordination-Driven Self-Assembly of Irregular Supramolecular Polygons. *J. Org. Chem.* **2009**, *74*, 3554–3557. (f) Sato, T.; Higuchi, M. An Alternately Introduced Heterometallo-Supramolecular Polymer: Synthesis and Solid-State Emission Switching by Electrochemical Redox. *Chem. Commun.* **2013**, *49* (46), 5256–5258. (g) Jurcek, O.; Bonakdarzadeh, P.; Kalenius, E.; Linnanto, J. M.; Groessl, M.; Knochenmuss, R.; Ihälainen, J. A.; Rissanen, K. Superchiral Pd_3L_6 Coordination Complex and Its Reversible Structural Conversion into $\text{Pd}_3\text{L}_3\text{Cl}_6$ Metallocycles. *Angew. Chem., Int. Ed.* **2015**, *54* (51), 15462–15467. (h) Liang, Y. P.; He, Y. J.; Lee, Y. H.; Chan, Y. T. Self-Assembly of Triangular Metallomacrocycles Using Unsymmetrical Bisterpyridine Ligands: Isomer Differentiation via TWIM Mass Spectrometry. *Dalton Trans.* **2015**, *44* (11), 5139–5145. (i) Wang, S.-Y.; Huang, J.-Y.; Liang, Y.-P.; He, Y.-J.; Chen, Y.-S.; Zhan, Y.-Y.; Hiraoka, S.; Liu, Y.-H.; Peng, S.-M.; Chan, Y.-T. Multicomponent Self-Assembly of Metallo-Supramolecular Macrocycles and Cagesthroughdynamic Heteroleptic Terpyridine Complexation. *Chem. - Eur. J.* **2018**, *24* (37), 9274–9284. (j) Ogata, D.; Yuasa, J. Dynamic Open Coordination Cage from Nonsymmetrical Imidazole-Pyridine Ditopic Ligands for Turn-On/Off Anion Binding. *Angew. Chem., Int. Ed.* **2019**, *58* (51), 18424–18428. (k) Sen, S. K.; Natarajan, R. Influence of Conformational Change and Interligand

Hydrogen Bonding in a Chiral Metal-Organic Cage. *Inorg. Chem.* **2019**, *58* (11), 7180–7188. (l) Zhang, X.; Dong, X.; Lu, W.; Luo, D.; Zhu, X.-W.; Li, X.; Zhou, X.-P.; Li, D. Fine-Tuning Apertures of Metal-Organic Cages: Encapsulation of Carbon Dioxide in Solution and Solid State. *J. Am. Chem. Soc.* **2019**, *141* (29), 11621–11627. (m) Preston, D.; Inglis, A. R.; Crowley, J. D.; Kruger, P. E. Self-Assembly and Cycling of a Three-State Pd_4L_4 Metallocsupramolecular System. *Chem. - Asian J.* **2019**, *14* (19), 3404–3408. (n) Wang, W.; Zhou, Z.; Zhou, J.; Shi, B.; Song, B.; Li, X.; Huang, F.; Stang, P. J. Self-Assembled Amphiphilic Janus Double Metallacycle. *Inorg. Chem.* **2019**, *58* (11), 7141–7145. (o) Pu, L.-M.; Yu, M.; Zhang, Y.; Long, H.-T.; Xu, W.-B.; Dong, W.-K. Tetrานuclear Cobalt(II) and Nickel(II) Complexes with an Unsymmetrical Salamo-Like Ligand: Structural Characterization, Hirshfeld Analysis and Fluorescent Properties. *Inorg. Chim. Acta* **2020**, *500*, 119238. (p) Lewis, J. E. M.; Tarzia, A.; White, A. J. P.; Jelfs, K. E. Conformational Control of Pd_2L_4 Assemblies with Unsymmetrical Ligands. *Chem. Sci.* **2020**, *11* (3), 677–683.

(21) (a) Suzuki, K.; Kawano, M.; Fujita, M. Solvato-Controlled Assembly of Pd_3L_6 and Pd_4L_8 Coordination "Boxes". *Angew. Chem., Int. Ed.* **2007**, *46* (16), 2819–2822. (b) Suzuki, K.; Tominaga, M.; Kawano, M.; Fujita, M. Self-Assembly of an M_6L_{12} Coordination Cube. *Chem. Commun.* **2009**, *13*, 1638–1640. (c) Zheng, Y.-R.; Zhao, Z.; Wang, M.; Ghosh, K.; Pollock, J. B.; Cook, T. R.; Stang, P. J. A Facile Approach toward Multicomponent Supramolecular Structures: Selective Self-Assembly via Charge Separation. *J. Am. Chem. Soc.* **2010**, *132* (47), 16873–16882. (d) Inokuma, Y.; Arai, T.; Fujita, M. Networked Molecular Cages as Crystalline Sponges for Fullerenes and Other Guests. *Nat. Chem.* **2010**, *2* (9), 780–783. (e) Clever, G. H.; Kawamura, W.; Tashiro, S.; Shiro, M.; Shionoya, M. Stacked Platinum Complexes of the Magnus' Salt Type inside a Coordination Cage. *Angew. Chem., Int. Ed.* **2012**, *51* (11), 2606–2609. (f) Harris, K.; Sun, Q.-F.; Sato, S.; Fujita, M. $M_{12}L_{24}$ Spheres with Endo and Exo Coordination Sites: Scaffolds for Non-Covalent Functionalization. *J. Am. Chem. Soc.* **2013**, *135* (34), 12497–12499. (g) Fu, J.-H.; Lee, Y.-H.; He, Y.-J.; Chan, Y.-T. Facile Self-Assembly of Metallo-Supramolecular Ring-in-Ring and Spiderweb Structures Using Multivalent Terpyridine Ligands. *Angew. Chem., Int. Ed.* **2015**, *54* (21), 6231–6235. (h) Sun, B.; Wang, M.; Lou, Z.; Huang, M.; Xu, C.; Li, X.; Chen, L.-J.; Yu, Y.; Davis, G. L.; Xu, B.; Yang, H.-B.; Li, X. From Ring-in-Ring to Sphere-in-Sphere: Self-Assembly of Discrete 2D and 3D Architectures with Increasing Stability. *J. Am. Chem. Soc.* **2015**, *137* (4), 1556–1564. (i) Roberts, D. A.; Pilgrim, B. S.; Cooper, J. D.; Ronson, T. K.; Zarra, S.; Nitschke, J. R. Post-Assembly Modification of Tetrazine-Edged $Fe^{II}L_6$ Tetrahedra. *J. Am. Chem. Soc.* **2015**, *137* (32), 10068–10071. (j) Castilla, A. M.; Ronson, T. K.; Nitschke, J. R. Sequence-Dependent Guest Release Triggered by Orthogonal Chemical Signals. *J. Am. Chem. Soc.* **2016**, *138* (7), 2342–2351. (k) Rizzuto, F. J.; Wu, W.-Y.; Ronson, T. K.; Nitschke, J. R. Peripheral Templation Generates an $M^{II}L_4$ Guest-Binding Capsule. *Angew. Chem., Int. Ed.* **2016**, *55* (28), 7958–7962. (l) Wang, S.-Y.; Fu, J.-H.; Liang, Y.-P.; He, Y.-J.; Chen, Y.-S.; Chan, Y.-T. Metallo-Supramolecular Self-Assembly of a Multicomponent Ditrigon Based on Complementary Terpyridine Ligand Pairing. *J. Am. Chem. Soc.* **2016**, *138* (11), 3651–3654. (m) Rizzuto, F. J.; Nitschke, J. R. Stereochemical Plasticity Modulates Cooperative Binding in a $Co^{II}L_6$ Cuboctahedron. *Nat. Chem.* **2017**, *9* (9), 903–908. (n) Rizzuto, F. J.; Wood, D. M.; Ronson, T. K.; Nitschke, J. R. Tuning the Redox Properties of Fullerene Clusters within a Metal-Organic Capsule. *J. Am. Chem. Soc.* **2017**, *139* (32), 11008–11011. (o) Yin, G.-Q.; Wang, H.; Wang, X.-Q.; Song, B.; Chen, L.-J.; Wang, L.; Hao, X.-Q.; Yang, H.-B.; Li, X. Self-Assembly of Emissive Supramolecular Rosettes with Increasing Complexity Using Multitopic Terpyridine Ligands. *Nat. Commun.* **2018**, *9* (1), 567. (p) Carpenter, J. P.; McTernan, C. T.; Ronson, T. K.; Nitschke, J. R. Anion Pairs Template a Trigonal Prism with Disilver Vertices. *J. Am. Chem. Soc.* **2019**, *141* (29), 11409–11413.

(22) (a) De Feyter, S.; Grim, P. C. M.; Esch, J. V.; Kellogg, R. M.; Feringa, B. L.; Schryver, F. C. D. Nontrivial Differentiation between Two Identical Functionalities within the Same Molecule Studied by STM. *J. Phys. Chem. B* **1998**, *102* (45), 8981–8987. (b) O'Sullivan, M.

C.; Sprafke, J. K.; Kondratuk, D. V.; Rinfray, C.; Claridge, T. D. W.; Saywell, A.; Blunt, M. O.; O'Shea, J. N.; Beton, P. H.; Malfois, M.; Anderson, H. L. Vernier Templating and Synthesis of a 12-Porphyrin Nano-Ring. *Nature* **2011**, *469* (7328), 72–75. (c) May, R.; Jester, S.-S.; Höger, S. A Giant Molecular Spoked Wheel. *J. Am. Chem. Soc.* **2014**, *136* (48), 16732–16735. (d) Kondratuk, D. V.; Perdigão, L. M. A.; Esmail, A. M. S.; O'Shea, J. N.; Beton, P. H.; Anderson, H. L. Supramolecular Nesting of Cyclic Polymers. *Nat. Chem.* **2015**, *7* (4), 317–322. (e) Shang, J.; Wang, Y.; Chen, M.; Dai, J.; Zhou, X.; Kuttner, J.; Hilt, G.; Shao, X.; Gottfried, J. M.; Wu, K. Assembling Molecular Sierpinski Triangle Fractals. *Nat. Chem.* **2015**, *7* (5), 389–93. (f) Zhang, Y.; Kersell, H.; Stefak, R.; Echeverria, J.; Iancu, V.; Perera, U. G. E.; Li, Y.; Deshpande, A.; Braun, K.-F.; Joachim, C.; Rapenne, G.; Hla, S.-W. Simultaneous and Coordinated Rotational Switching of All Molecular Rotors in a Network. *Nat. Nanotechnol.* **2016**, *11* (8), 706–712. (g) Gu, J.-Y.; Cai, Z.-F.; Wang, D.; Wan, L.-J. Single-Molecule Imaging of Iron-Phthalocyanine-Catalyzed Oxygen Reduction Reaction by *in Situ* Scanning Tunneling Microscopy. *ACS Nano* **2016**, *10* (9), 8746–8750. (h) Mo, Y.; Chen, T.; Dai, J.; Wu, K.; Wang, D. On-Surface Synthesis of Highly Ordered Covalent Sierpiński Triangle Fractals. *J. Am. Chem. Soc.* **2019**, *141* (29), 11378–11382. (i) Wang, X.; Cai, Z.-F.; Wang, Y.-Q.; Feng, Y.-C.; Yan, H.-J.; Wang, D.; Wan, L.-J. *In Situ* Scanning Tunneling Microscopy of Cobalt-Phthalocyanine-Catalyzed CO_2 Reduction Reaction. *Angew. Chem., Int. Ed.* **2020**, *59* (37), 16098–16103. (j) Zhang, Z.; Li, Y.; Song, B.; Zhang, Y.; Jiang, X.; Wang, M.; Tumbleston, R.; Liu, C.; Wang, P.; Hao, X.-Q.; Rojas, T.; Ngo, A. T.; Sessler, J. L.; Newkome, G. R.; Hla, S.-W.; Li, X. Intra- and Intermolecular Self-Assembly of a 20-nm-Wide Supramolecular Hexagonal Grid. *Nat. Chem.* **2020**, *12* (5), 468–474. (k) Wang, L.; Song, B.; Li, Y.; Gong, L.; Jiang, X.; Wang, M.; Lu, S.; Hao, X.-Q.; Xia, Z.; Zhang, Y.; Hla, S.-W.; Li, X. Self-Assembly of Metallo-Supramolecules under Kinetic or Thermodynamic Control: Characterization of Positional Isomers Using Scanning Tunneling Spectroscopy. *J. Am. Chem. Soc.* **2020**, *142* (21), 9809–9817.

(23) (a) Newkome, G. R.; Wang, P.; Moorefield, C. N.; Cho, T. J.; Mohapatra, P. P.; Li, S.; Hwang, S.-H.; Lukyanova, O.; Echegoyen, L.; Palagallo, J. A.; Iancu, V.; Hla, S.-W. Nanoassembly of a Fractal Polymer: A Molecular "Sierpinski Hexagonal Gasket". *Science* **2006**, *312* (5781), 1782–1785. (b) Zhang, Z.; Wang, H.; Wang, X.; Li, Y.; Song, B.; Bolarinwa, O.; Reese, R. A.; Zhang, T.; Wang, X.-Q.; Cai, J.; Xu, B.; Wang, M.; Liu, C.; Yang, H.-B.; Li, X. Supersnowflakes: Stepwise Self-Assembly and Dynamic Exchange of Rhombus Star-Shaped Supramolecules. *J. Am. Chem. Soc.* **2017**, *139* (24), 8174–8185. (c) Song, B.; Kandpal, S.; Gu, J.; Zhang, K.; Reese, A.; Ying, Y.; Wang, L.; Wang, H.; Li, Y.; Wang, M.; Lu, S.; Hao, X.-Q.; Li, X.; Xu, B.; Li, X. Self-Assembly of Polycyclic Supramolecules Using Linear Metal-Organic Ligands. *Nat. Commun.* **2018**, *9* (1), 4575. (d) Wang, L.; Liu, R.; Gu, J.; Song, B.; Wang, H.; Jiang, X.; Zhang, K.; Han, X.; Hao, X.-Q.; Bai, S.; Wang, M.; Li, X.; Xu, B.; Li, X. Self-Assembly of Supramolecular Fractals from Generation 1 to 5. *J. Am. Chem. Soc.* **2018**, *140* (43), 14087–14096. (e) Wang, H.; Li, Y.; Yu, H.; Song, B.; Lu, S.; Hao, X.-Q.; Zhang, Y.; Wang, M.; Hla, S.-W.; Li, X. Combining Synthesis and Self-Assembly in One Pot to Construct Complex 2D Metallo-Supramolecules Using Terpyridine and Pyrlyium Salts. *J. Am. Chem. Soc.* **2019**, *141* (33), 13187–13195. (f) Li, Y.; Huo, G.-F.; Liu, B.; Song, B.; Zhang, Y.; Qian, X.; Wang, H.; Yin, G.-Q.; Filosa, A.; Sun, W.; Hla, S. W.; Yang, H.-B.; Li, X. Giant Concentric Metallosupramolecule with Aggregation-Induced Phosphorescent Emission. *J. Am. Chem. Soc.* **2020**, *142* (34), 14638–14648.

(24) Chan, Y.-T.; Li, X.; Yu, J.; Carri, G. A.; Moorefield, C. N.; Newkome, G. R.; Wesdemiotis, C. Design, Synthesis, and Traveling Wave Ion Mobility Mass Spectrometry Characterization of Iron(II)- and Ruthenium(II)-Terpyridine Metallomacrocycles. *J. Am. Chem. Soc.* **2011**, *133* (31), 11967–11976.

(25) (a) Kanu, A. B.; Dwivedi, P.; Tam, M.; Matz, L.; Hill, H. H., Jr. Ion Mobility-Mass Spectrometry. *J. Mass Spectrom.* **2008**, *43* (1), 1–22. (b) Chan, Y.-T.; Li, X.; Soler, M.; Wang, J.-L.; Wesdemiotis, C.; Newkome, G. R. Self-Assembly and Traveling Wave Ion Mobility Mass Spectrometry Analysis of Hexacadmium Macrocycles. *J. Am. Chem. Soc.*

2009, 131 (45), 16395–16397. (c) Brocker, E. R.; Anderson, S. E.; Northrop, B. H.; Stang, P. J.; Bowers, M. T. Structures of Metallosupramolecular Coordination Assemblies Can Be Obtained by Ion Mobility Spectrometry-Mass Spectrometry. *J. Am. Chem. Soc.* 2010, 132 (38), 13486–13494. (d) Ujma, J.; De Cecco, M.; Chepelin, O.; Levene, H.; Moffat, C.; Pike, S. J.; Lusby, P. J.; Barran, P. E. Shapes of Supramolecular Cages by Ion Mobility Mass Spectrometry. *Chem. Commun.* 2012, 48 (37), 4423–4425.

(26) Li, Z.; Li, Y.; Zhao, Y.; Wang, H.; Zhang, Y.; Song, B.; Li, X.; Lu, S.; Hao, X.-Q.; Hla, S.-W.; Tu, Y.; Li, X. Synthesis of Metallocopolymers and Direct Visualization of the Single Polymer Chain. *J. Am. Chem. Soc.* 2020, 142 (13), 6196–6205.

(27) (a) Chen, L.-J.; Zhao, G.-Z.; Jiang, B.; Sun, B.; Wang, M.; Xu, L.; He, J.; Abliz, Z.; Tan, H.; Li, X.; Yang, H.-B. Smart Stimuli-Responsive Spherical Nanostructures Constructed from Supramolecular Metalloendrimers via Hierarchical Self-Assembly. *J. Am. Chem. Soc.* 2014, 136 (16), 5993–6001. (b) Ludlow, J. M.; Saunders, M. J.; Huang, M.; Guo, Z.; Moorefield, C. N.; Cheng, S. Z. D.; Wesdemiotis, C.; Newkome, G. R. Amphiphilic [Tpy-M^{II}-Tpy] Metallotriangles: Synthesis, Characterisation and Hierarchical Ordering. *Supramol. Chem.* 2017, 29 (1), 69–79.